Bipolar charge redistribution in resonant-tunneling light-emitting diodes

C. Van Hoof and J. Genoe
Interuniversity Microelectronics Center (IMEC), Kapeldreef 75, B-3001 Leuven, Belgium

D. Bertram
Max-Planck Institut für Festkörperforschung Heisenbergstrasse 1, D-70569 Stuttgart, Germany

H.T. Grahn
Paul-Drude Institut für Festkörperelektronik Hausvogteiplatz 5-7, D-10117 Berlin, Germany

G. Borghs
Interuniversity Microelectronics Center (IMEC), Kapeldreef 75, B-3001 Leuven, Belgium
(Received 4 August 1994)

Resonant-tunneling light-emitting diodes contain three regions where charges accumulate during device operation: the electron and hole accumulation layer in the emitter and collector, respectively, and the quantum well of the structure for bipolar accumulation. It is shown that charges redistribute over these regions with increasing current through the device and that the amount of redistribution depends on tunneling escape rate and hence on the thickness of the tunneling barriers. This charge redistribution is particularly pronounced at the resonances in the current-voltage characteristics. The process is clarified by electroluminescence spectroscopy on a set of resonant-tunneling light-emitting diodes with different barrier thickness. Signal intensities from the three spectral regions are compared and yield the relative majority carrier occupation of each region. A tradeoff in quantum-well versus accumulation-layer emission is observed as the tunneling escape rate increases with decreasing barrier thickness. Line-shape analysis yields free-carrier electron and hole broadening in the quantum well. Peak position analysis allows the determination of the electric field across the well region from which an accurate picture of the band bending during tunneling is obtained.

I. INTRODUCTION

Resonant-tunneling light-emitting diodes (RTLED's) are p-i-n diodes containing a double-barrier (or multibarrier) resonant-tunneling structure in the intrinsic region of the diode.[1–7] The simultaneous intraband tunneling of electrons and heavy holes gives rise to injection electroluminescence from the quantum well and from the two accumulation layers on either side of the resonant-tunneling structure. The fast quantum-well tunnel escape time obtained in these structures allows us to obtain a fast response of the optical output[8] otherwise only found in semiconductor lasers. As the external bias sweeps across a region of resonant tunneling, either by electrons or by holes, the current shows a resonance and intuitively a resonance in light output intensity is expected. This was observed in the first reported RTLED's. This, however, is not necessarily the case, because (i) the injection of electrons and holes is not mutually independent, and (ii) the discrepancy in the amounts of electrons and holes will lead to a light output that is governed by the number of minority carriers in the structure.

The aim of this paper is to substantiate both of the above statements by performing a more complete investigation of RTLED's. We will show that the requirement of conserving external total bias and/or band bending between resonance and off-resonance will translate in an electron and hole redistribution in the quantum well and in both accumulation layers, an effect we will call *charge feedback*. This feedback mechanism will alter the light output from the three emission regions. The argument of different electron versus hole currents, which will be substantiated from the electrical characteristics, causes the presence of a minority carrier hole flow. If the discrepancy with the electron flow is very large, the light output versus current will be entirely hole dependent and will not follow the electron resonances.

The effects will be studied by comparing the characteristics of three RTLED's that only differ in the width of the tunneling barriers. As a consequence, emission energies do not vary, but the current scales exponentially with barrier thickness.

II. EXPERIMENT

Three p-i-n samples were grown by molecular-beam epitaxy on p^+-doped GaAs substrates and consisted of the following layers : 300-nm GaAs p^+ (4×10^{18} cm^{-3}) buffer layer, 50-nm GaAs not intentionally doped (NID) spacer layer, the resonant-tunneling structure, 50-nm GaAs NID spacer layer, and a 300-nm GaAs n^+ (2×10^{18} cm^{-3}) top contact layer. The resonant-tunneling structure had a 5-nm GaAs quantum well and 5-nm, 4-

0163-1829/95/51(19)/13491(8)/$06.00 ©1995 The American Physical Society

nm, and 3-nm AlAs barriers for samples B5, B4, and B3, respectively. Standard optical lithography was used to define rectangular mesas of 150 × by 100 μm^2 and AuGe/Ni/Au ohmic contacts featuring a 100-μm side optical window on top of the mesa. The sample is mounted into a chip carrier, which is placed on the cold finger of a liquid nitrogen dewar in order to maintain a temperature of about 85 K during the experiments.

The calculated band structure of the device at flat band (approximately 1.5 V) and the corresponding electron and hole subbands are shown in Fig. 1. The calculated confinement energies are shown in the inset adding up to transition energies for the electron to heavy-hole transition $E1$-HH1 = 1.613 eV and the electron to light-hole transition $E1$-LH1 = 1.647 eV. They agree with the measured electroluminescence spectral data to well within 1 ML thickness variation, which would result in a 8-meV shift in transition energy of $E1$-HH1.

The electroluminescence signal emitted in forward bias is dispersed in a 0.32-m spectrometer and the resulting spectrum is imaged onto a cooled charge-coupled device (CCD) array. The voltage range under investigation covers the lowest electron and hole resonances in forward bias.

III. ELECTRICAL CHARACTERIZATION

The current-voltage characteristics at 85 K of the three RTLED's beyond flat band show the presence of resonances (Fig. 2), of which the smaller ones are due to light-hole resonant tunneling and the larger are due to electron resonant tunneling. The relative positions are compatible with the energy-level calculations shown in the inset of Fig. 2 where the calculated transmission coefficient of electrons, light-holes, and heavy holes is plotted for sample B4. With increasing bias successively the bottom light-hole, electron, and second light-hole resonances are obtained. Heavy-hole resonances are not observed in the $I(V)$ at 85 K. With decreasing barrier thickness from B5 to B3, the currents through the device exponentially increase, which in turn increases the positions of the resonances because of the increasing voltage drop across the contact resistance. Subtracting this voltage drop by assuming a series resistance of 10 Ω makes the corresponding light-hole and electron resonances of the three samples coincide. The series resistance is responsible for the observed current hysteresis in B3.

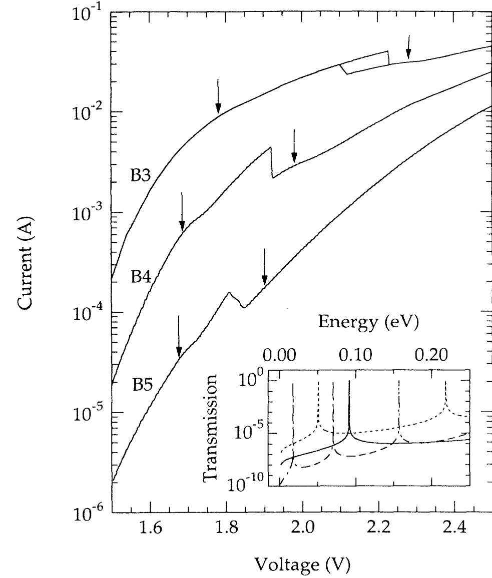

FIG. 2. Current-voltage characteristics of the three RTLED's at 85 K, with barriers of 5 nm (B5, bottom), 4 nm (B4, middle), and 3 nm (B3, top). The larger resonances are are due to electron resonant tunneling and the smaller (indicated by arrows) are light-hole resonances. The shift of the resonances to higher voltage with decreasing barrier thickness is due to the increased voltage drop across the contact resistance. The inset shows the transmission coefficient of the different carriers; electrons (solid line), light holes (dashed line), and heavy holes (long dashes) through the RTLED for sample B4 as a function of carrier energy.

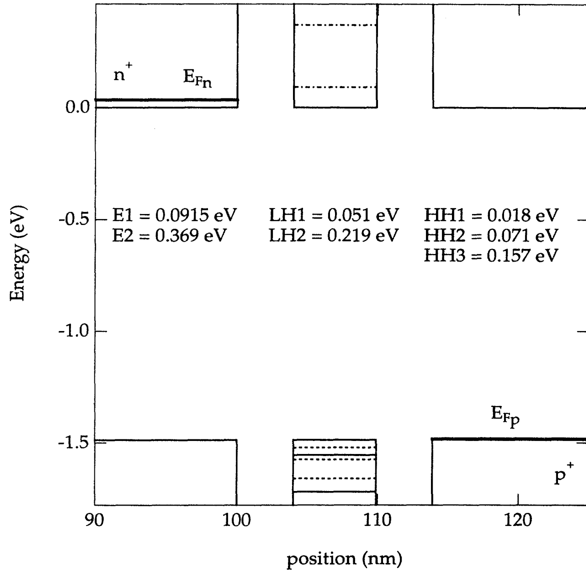

FIG. 1. Band structure of the bipolar RTLED at flat band (1.50 V across the structure) over the energy range of the lower electron and hole subbands. The Fermi levels in the n- and p-doped contact regions are added as bold lines. Electron subbands (dot-dashed lines), light hole (solid lines), and heavy hole (dashed lines) are added and the confinement energies are given.

This does not explain why the second light-hole resonance in Fig. 2 is much closer to the first electron resonance than follows from the energy spacing in the inset of Fig. 2. Self-consistent band-structure calculations for the three samples (Fig. 3) resolve this apparent disagreement. The band-bending profiles of the three samples were calculated for the devices biased at the electron resonance. Since the net quantum-well charge at all bias values beyond the onset of electron tunneling is not zero but negative, the electric field E across the well is not constant but gradually increases towards the bottom, as

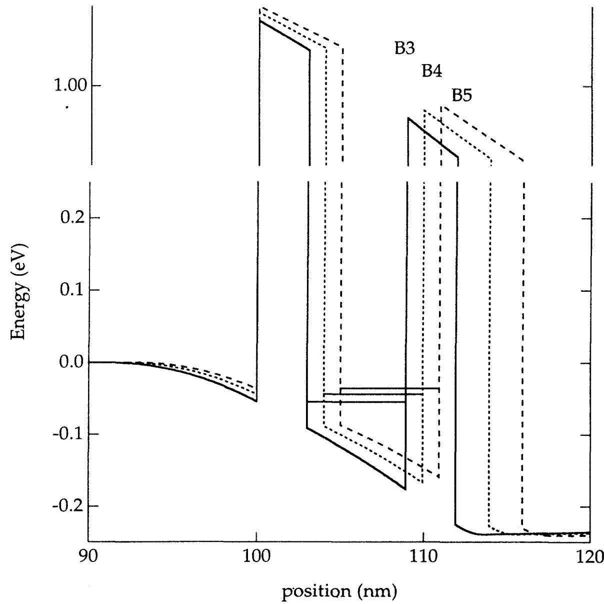

FIG. 3. Calculated band bending at the electron resonance for B3 (solid line), B4 (dashed line), and B5 (long dashes). From the slope of the barrier potential follows that the bottom barrier on the hole accumulation layer side acquires most band bending. A bias scan, therefore, sweeps through the electron and hole energy subbands at different rate. The electric field at resonance decreases from B3 over B4 to B5 because the same voltage drops over a wider device.

can be seen from the different slopes of the top and bottom barrier potential. Since the electric field across the bottom barrier is higher than that across the top barrier, the holes enter the tunneling structure at higher energy ($E_{\text{bottom barrier}} \times d_{\text{barrier}}$) than the electrons ($E_{\text{top barrier}} \times d_{\text{barrier}}$). The valence-band resonances are, therefore, shifted to lower bias with respect to the tunneling transmission calculations as indeed observed in the $I(V)$. This reasoning also suggests that electron and light-hole resonances may even coincide depending on the relative charging of the quantum well and the accumulation layers. This can be achieved by correct tuning of the well and barrier widths

The band-bending diagrams in Fig. 3 are plotted at the electron resonance, as can be seen from the alignment of the conduction band in the emitter with the electron subband in the quantum well. The external bias at the electron resonance is the same for the three samples. This holds because the equal well width results in identical electron subband energies E_{electron} and the resonant voltage is approximately 2 $\times E_{\text{electron}}$ (which is exact if the well were fully depleted). Since the barrier widths are different, the resonant electric field across the quantum well increases with decreasing barrier thickness (same voltage drop over a narrower structure), from 120 kV/cm (B5) over 140 kV/cm (B4) to 160 kV/cm (B3). The optical experiments from Sec. IV will substantiate this calculation.

The relative intensity of hole versus electron resonances remains to be explained. The near equal doping concentration of the n- and p- doped layers results in equal free-carrier concentrations but, because of the different effective density of states ($N_c = 4.7 \times 10^{17}$ cm^{-3} and $N_v = 7.0 \times 10^{18}$ cm^{-3}), the electron Fermi level in the electron accumulation layer is larger than the hole Fermi level in the accumulation layer. This holds for all forward bias values. The heavy-hole concentration outnumbers the light-hole concentration by the ratio of the density of states effective masses, i.e., $(m^*_{\text{hh}})^{3/2}/(m^*_{\text{lh}})^{3/2} \approx 11$. This assumes constant effective masses and no valence-band mixing and is, therefore, only valid as first approximation. Charge neutrality thus requires that the amount of electrons, light holes, and heavy holes N_e:N_{lh}:N_{hh} around the resonant tunneling structure is 12:1:11. Theory on unipolar n-type resonant-tunneling structures establishes that the peak resonant carrier current is proportional to the integral under the transmission resonance times the carrier effective mass times the carrier Fermi energy.[9] The integrated transmission (IT) for electrons, light holes, and heavy holes IT_e:IT_{lh}:IT_{hh} for the three structures relates as 0.3:1:10^{-3}. By further neglecting the difference in Fermi distribution between electrons and holes, the relative electron, light-hole, and heavy-hole resonant peak currents relate as 3:1:5$\times 10^{-2}$. The last approximation results in an overestimate of the hole currents. These relative electron and light-hole currents are consistent with the experimental observations (Fig. 2) and prove the absence of heavy-hole resonances in the $I(V)$.

The current peak-to-valley ratio of the electron resonance at 85 K does not decrease with increasing barrier thickness, since the resonant and nonresonant-tunneling currents decrease with increasing barrier thickness and the thermionic current is small at this temperature. Nevertheless the overall peak-to-valley ratio of all resonances in these bipolar structures is smaller than in the corresponding unipolar n-or p-type structures because of the double component of the two nonresonant currents (electrons and holes). Because of the lower valence-band barrier, the thermionic light-hole current and the nonresonant light-hole current are even larger than the corresponding electron currents.

IV. SPECTRAL CHARACTERIZATION

A. Spectra

The normalized electroluminescence spectra beyond the onset of the bottom light-hole resonance are shown in Fig. 4 for the three samples (solid line for B5, dashed for B4, and dot-dashed for B3). Beyond 1.5 V an electron and hole tunneling current flows giving rise to emission from the n-GaAs (at 1.507 eV) and p-GaAs (at 1.485 eV) contact regions that can be distinguished spectrally because the combined effects of band-filling and band-gap narrowing are positive for n-doped GaAs and negative for p-doped GaAs.[10] Most of the emission from these two regions stems from the accumulation layers very close to the resonant-tunneling structure since the charge density is highest.

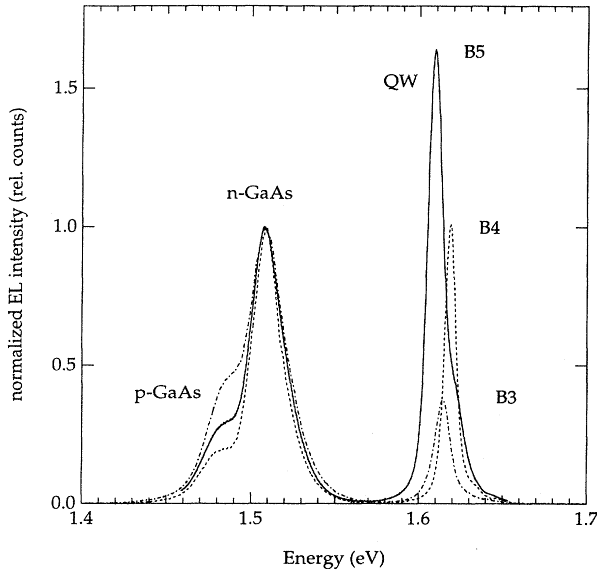

FIG. 4. Electroluminescence spectra at 85 K beyond flat band for B5 (solid line), B4 (dotted line), and B3 (dot-dashed line) normalized to identical n-GaAs emission. With decreasing barrier thickness the quantum-well intensity decreases because of the increased tunneling rate.

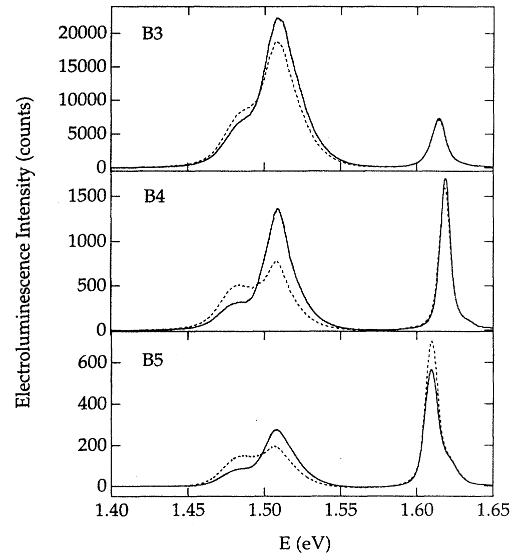

FIG. 5. Electroluminescence spectra at 85 K at (solid line) and beyond (dashed line) the first light-hole resonance for B5 (bottom), B4 (middle), and B3 (top). Charge redistribution is apparent from the change of the accumulation-layer signals.

Even though the hole current consists mainly of light-holes entering the resonant tunneling structure, fast intersubband relaxation to the bottom heavy-hole subband will occur and the main quantum-well electroluminescence feature will be the electron to heavy-hole transition (at $\approx$ 1.613 eV) and a smaller feature arises from electron to light-hole transitions (at $\approx$ 1.647 eV). Because the tunneling escape time decreases with decreasing barrier thickness, the relative quantum-well versus GaAs emission decreases (Fig. 4) from 1.7 over 1.0 to 0.35. These values do not linearly translate into tunneling escape time ratios because the radiative recombination rate is a complex function of electron and light- and heavy-hole tunneling times. Transient photoluminescence can resolve the tunneling escape times as has been demonstrated on a unipolar triple-barrier structure.[11]

B. Charge distribution and charge feedback

A complete bias scan of the spectral emission lines is provided below but we start with two snapshots of the spectra at and off-resonance for the ground-state electron and light-hole subbands.

Electroluminescence spectra at and beyond the ground light-hole resonance are very similar for the three samples (Fig. 5). At resonance (solid line in Fig. 5) the n-GaAs emission is larger than the p-GaAs emission, but beyond the resonance the n-GaAs signal has decreased and the p-GaAs signal has increased. The decreased n-GaAs emission obviously reflects a decreasing hole current, even though the total current does not decrease at this resonance (cf., Fig. 2). The p-GaAs emission increase is helped by two factors: the concentration in the hole accumulation layer increases since tunneling of holes through the structure is blocked and the total net charge around the structure has to remain zero. Second, the off-resonance hole voltage is several MV closer to the electron resonance and, therefore, the electron current has increased. Both effects cannot be distinguished but the bias dependence of the quantum-well (QW) emission substantiates the presence of both. For B5, the QW emission increases beyond resonance, demonstrating the increased electron current and the fact that the hole recombination efficiency is not unity or else the emission would not increase. B4 and B3 in contrast show an albeit small decrease in QW emission (much less than the decrease in n-GaAs emission) reflecting, therefore, the decrease in hole concentration in the well. Since the decrease is smaller than that of the n-GaAs emission, it is counteracted by an increased electron population, an effect that cannot occur for the n-GaAs emission since it only requires one free carrier.

At the electron resonance, the p-GaAs emission has increased with respect to the n-GaAs emission and has even become larger for B5 and B4 (Fig. 6). This reflects the resonantly increased electron current. The n-GaAs emission in contrast has increased far less since the hole occupation is not resonantly enhanced and more holes are lost to the quantum well for recombination. Off-resonance, the n-GaAs emission has doubled (for B5 and B4) or tripled (for B3) and the p-GaAs emission is more than halved. The quantum-well emission always decreases off-resonance and this decrease is 0.9 (B5), 0.5 (B4), and 0.7 (B3). The decrease (for QW and p-GaAs) reflects the loss of electrons in the quantum-well off-resonance and the decrease in the total electron current. This loss has to be countered by an increase of the electron occupation in the electron accumulation layer to conserve external band bending. This charge feedback pulls the n-GaAs

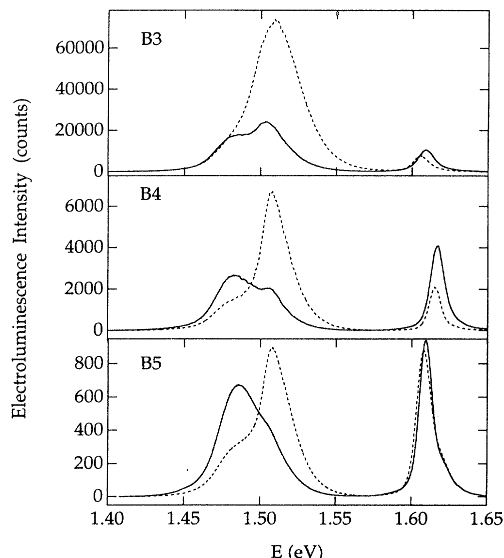

FIG. 6. Electroluminescence spectra at 85 K at (solid line) and beyond (dashed line) the first electron resonance for B5 (bottom), B4 (middle), and B3 (top). Charge feedback is apparent from the strong increase in n-GaAs emission off-resonance compensating for the loss of electron charge in the quantum well.

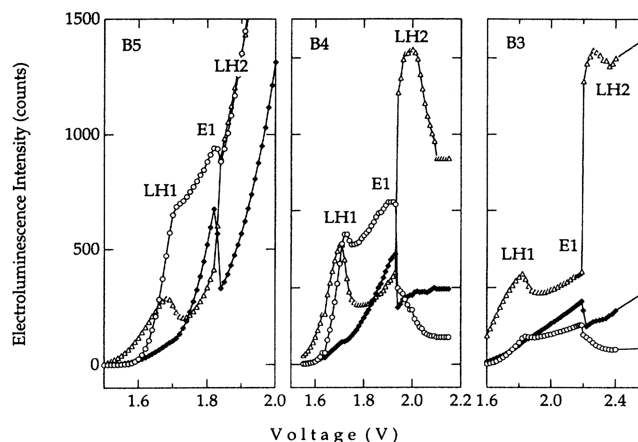

FIG. 7. Electroluminescence intensity vs bias of the three emission lines for B5 (left), B4 (middle), and B3 (right). Triangles (diamonds, circles) indicate the n-GaAs (p-GaAs, quantum-well), emission, respectively. The origin of the resonances is indicated on the graphs. Charge feedback is prominent at the electron resonance.

accumulation-layer concentration up and causes the apparent increase in n-GaAs emission. Similarly to the discussion of the hole resonance, the switching to off electron resonance increases the band bending across the quantum well and the second barrier, and brings the structure closer to the second hole resonanc; thereby, increasing the hole current and hence the hole occupation. This cannot be the only effect since it cannot provide charge neutrality across the whole structure. The presence of this effect is proven by the shift of the quantum-well emission to lower energy due to the quantum-confined Stark effect.

A complete picture is given in Fig. 7 where the bias dependence of all emission lines is plotted for the three samples. The n-GaAs emission line (triangles in Fig. 7) peaks at the light-hole resonance (cf., Fig. 5) and reaches a minimum off-resonance, beyond which it increases with current. At the second light-hole resonance it peaks again and becomes minimum off-resonance. This second light-hole resonance is pronounced for B4 and B3. The n-GaAs emission, therefore, follows the hole current through the device. The switch from electron resonance to off-resonance strongly redistributes electron charge between the quantum well and accumulation layer and because of the increased electron concentration in the accumulation layer the n-GaAs emission drastically increases (cf., Fig. 6). Therefore, also the changing population of the electron reservoir is monitored. From sample-to-sample the amount of charge feedback increases with decreasing barrier thickness because a larger charge is needed to conserve band bending. The p-GaAs emission line (diamonds in Fig. 7) peaks at the electron resonance and becomes minimum off-resonance so it follows indeed the electron current through the device. The small variations at the hole resonances are strictly due to the n-GaAs background superimposed on the p-GaAs emission line. Because of the much smaller hole current, charge feedback effects that change the hole reservoir are negligible. The intensity variations of n- and p-accumulation layers, therefore, monitor the minority carriers.

C. Quantum-well charge accumulation

Since the quantum-well emission (circles in Fig. 7) stems from recombination of tunneling electrons and tunneling holes, it should follow both current variations. This is clearly observed at all resonances for B4 and B3. For these samples, the combined effect of electrons and light holes switching to off-resonance leads to a maximum optical on-off ratio. This implies that for device applications coinciding electron and hole resonances are essential. B5 in contrast shows much smaller variations of the quantum-well intensity at the resonances in spite of the strong electron and hole current resonances as witnessed from n- and p-GaAs intensity variations. (This implies that the quantum efficiency for recombination in the quantum well is not unity for electrons nor for holes and the decreasing electron occupation is counteracted by an increasing hole population. The line shape of the quantum-well emission resolves the relative importance of either carrier for the three samples. Figure 8 shows the full width half at maximum (FWHM) of the quantum-well line. The extraction of the carrier concentration[12] from line-shape analysis has already been shown by photoluminescence on unipolar n-type[13–16] and p-type[17,18] resonant-tunneling structures. The behavior of B5 is opposite that of B4 and B3: for B5 the change in free-carrier hole broadening between on- and off-resonance is six times (three times) more pronounced than for B4 (B3) proving that for the two-dimensional system more holes occupy the structure. Since the escape time for B5

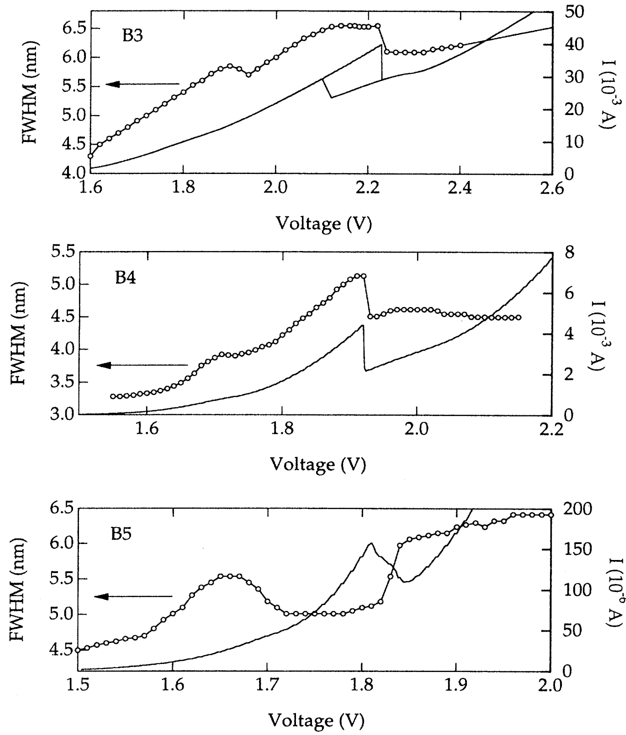

FIG. 8. FWHM of the quantum-well emission line for B5 (bottom), B4 (middle), and B3 (top) vs bias. The $I(V)$ characteristics are added for clarity. In B5, free-carrier hole broadening is dominant. For the thinner barrier samples, free-carrier electron broadening dominates the hole broadening because of the lower hole to electron quantum-well occupation. B5 shows the presence of bipolar charge feedback: beyond the electron resonance where the electron current decreases the hole current increases.

is largest, the heavy holes do not escape until they radiatively recombine leading to a very strong hole charge buildup. At the electron resonance where the electron occupation decreases, the hole population increases as substantiated in the beginning of this section. This is apparent from the linewidth increase of B5 at the electron resonance. B4 and B3 show linewidth reductions at the electron resonance proving that the main carrier change responsible for the intensity profile is the electron charge reduction. Besides slow escape, an additional reason for the opposite behavior of B5 may be scattering in the thick barriers leading to a population of the subbands also off-resonance. Also, the lower relative resonant-tunneling current with respect to the nonresonant-tunneling current creates a bipolar population in the well at all bias values.

The electric field across the quantum well is monitored from the red shift of the emission line (Fig. 9). The shift is quadratic for samples B5 and B4 and superlinear for B3. The latter is due to the voltage drop across the series resistance, which stretches the voltage axis. As the barrier thickness decreases, the resonances are obtained at increased electric fields, which is in agreement with theory as calculated in Fig. 3. From resonance to off-resonance,

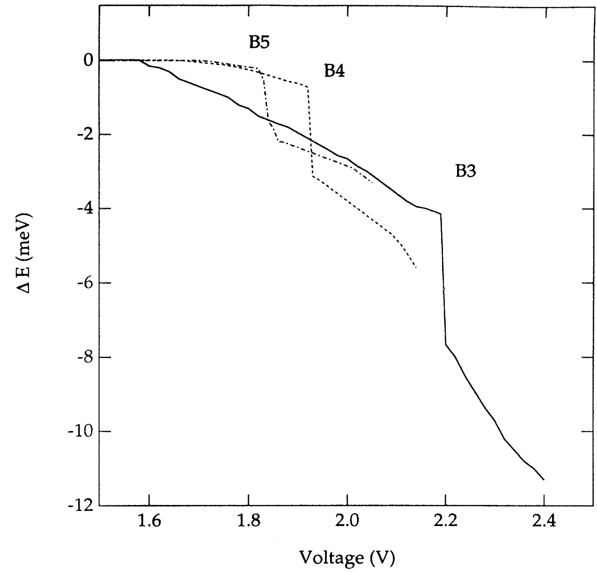

FIG. 9. Red shift of the quantum-well emission with increasing electric field for B5 (dot-dashed line), B4 (dashed line), and B3 (solid line). For decreasing barrier thickness, the resonances are obtained at increased electric fields as calculated in Fig. 3. As the quantum well is depleted of electrons beyond the electron resonance, the electric field increases. This increased band bending is responsible for an increased hole current off-resonance.

the electric field increases since the quantum well is depleted of electrons and assumes a larger field. This increased band bending is responsible for an increased hole current off-resonance as explained in Sec. III.

D. Optical power output

The narrow quantum-well emission is the useful emission line, but because of the non-negligible contact-layer emission, the total emitted power can be considered, from which a total quantum efficiency can be extracted (Fig. 10). The bottom graph in Fig. 10 shows the power emitted by the sample (dashed line) versus scaled voltage. The voltage drop across the series resistance has been subtracted from the externally applied voltage so as to remove resistive heating from the argument. The main variations in power output stem from hole resonances and very little effect is due to the electron resonance. This substantiates the reasoning under Sec. III (electrical characterization) where we calculated the relative electron versus hole currents through the device. With decreasing barrier width, the optical power output exponentially increases and follows the overall slope of the $I(V)$. The optical power output at the electron resonance for B5 (B4, B3) is 1.10 μW (22.1 μW, 153.0 μW) and off-resonance 1.15 μW (28.8 μW, 233.0 μW). Dividing the emitted power by the consumed electrical power yields the quantum efficiency (top graph in Fig. 10). Local maxima are again obtained at the hole resonances and the quantum efficiency steps up at the electron resonance.

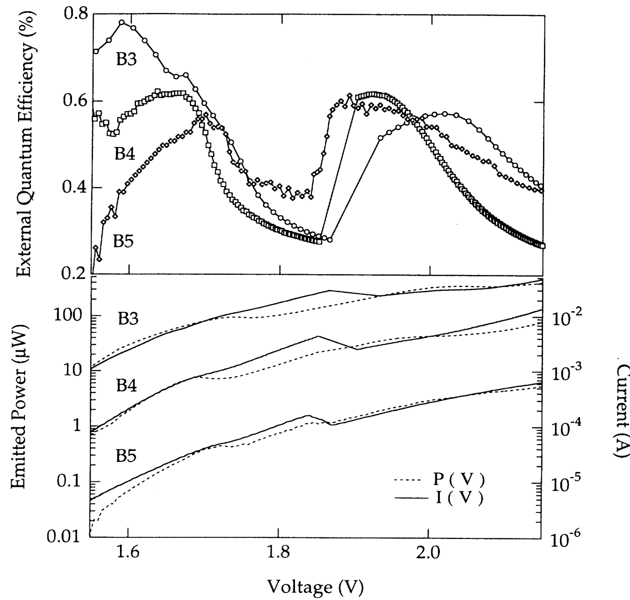

FIG. 10. Optical power output (dashed line in bottom graph) and external optical quantum efficiency (top graph) vs scaled voltage. The current-voltage characteristics have been added as single lines in the bottom graph. The voltage drop across the series resistance has been subtracted from the voltage scale so as to remove resistive heating from the picture. Local extrema are obtained at the hole resonances and the quantum efficiency is minimum at the electron resonance indicating the discrepancy between the numbers of holes and electrons.

This seemingly illogical step is obtained because the optical output relies on the smaller hole current, whereas the electrical current at the electron resonance is mostly an electron current. Total quantum efficiency is, therefore, not a good measure for the efficiency of RTLED's because of the large discrepancy between electron and hole tunneling currents.

From the electrical and spectral characterization and their discussion, we can summarize several suggestions that will lead to improved device performance, i.e, higher absolute electroluminescence intensity and maximized on-off ratios. Wide-barrier samples are best for larger relative quantum-well emission versus contact-layer emission, but have a low optical on-off ratio. Narrower barrier samples have better optical on-off ratios, and lead to fast switch-on and switch-off, but the relative quantum-well emission is lower. Due to the charge buildup in the narrower-barrier samples, the excited light-hole resonance is very close to the electron resonance, which in effect maximizes the optical on-off ratio because both populations go off-resonance. Whereas the speed of these devices depends on electron escape, the holes in the narrower-barrier devices limit the optical power output of the devices.

V. CONCLUSIONS

In conclusion, electrical and optical characteristics of resonant-tunneling light-emitting diodes have been presented and analyzed. The presence of a charge feedback mechanism that guarantees self-consistency between resonance and off-resonance has been witnessed. This complex charge distribution versus bias has been clarified and it is shown that electrons and holes redistribute over the accumulation layers with increasing current through the device and that the amount of redistribution depends on tunneling escape rate and hence on the thickness of the tunneling barriers. This charge redistribution is particularly pronounced at the resonances in the current-voltage characteristics. Signal intensities from the three spectral regions are compared and yield the relative majority carrier occupation of each region. A tradeoff in quantum-well versus accumulation-layer emission is observed as the tunneling escape rate increases with decreasing barrier thickness. Line-shape analysis yields free-carrier electron and hole broadening in the quantum well. Peak position analysis allows the determination of the electric field across the well region from which an accurate picture of the band bending during tunneling is obtained.

ACKNOWLEDGMENTS

We thank E. Goovaerts for valuable discussions. This work was supported by the European Community ESPRIT Project No. 7193 PARTNERS. Financial support is gratefully acknowledged from the Belgian National Fund for Scientific Research (NFWO) for one of the authors (C.V.H.).

[1] C. Van Hoof, J. Genoe, R. Mertens, G. Borghs, and E. Goovaerts, Appl. Phys. Lett. **60**, 77 (1992).

[2] C. Van Hoof, J. Genoe, S. Raymond, and G. Borghs, Appl. Phys. Lett. **63**, 2390 (1993).

[3] D. Bertram, H. Lage, H.T. Grahn, and K. Ploog, Appl. Phys. Lett. **64**, 1012 (1994).

[4] P.D. Buckle, J.W. Cockburn, R.J. Teissier, A.R.K. Willcox, D.M. Whittaker, M.S. Skolnick, G.W. Smith, R. Grey, G. Hill, and M.A. Pate, Semicond. Sci. Technol. **9**, 533 (1994).

[5] H.T. Grahn, D. Bertram, H. Lage, K. von Klitzing, and K. Ploog, Semicond. Sci. Technol. **9**, 537 (1994).

[6] D.K. Maude, O. Kuhn, J.C. Portal, M. Henini, L. Eaves, G. Hill, and M.A. Pate, Semicond. Sci. Technol. **9**, 540 (1994).

[7] H.B. Evans, L. Eaves, and M. Henini, Semicond. Sci. Technol. **9**, 555 (1994).

[8] C. Van Hoof, J. Genoe, R. P. Mertens, E. Goovaerts, and G. Borghs, Electron. Lett. **28**, 123 (1992).

[9] P. Guéret, C. Rossel, E. Marclay, and H. Meier, J. Appl. Phys. **66**, 278 (1989).

[10] G. Borghs, K. Bhattacharya, K. Deneffe, P. Van Mieghem, and R. Mertens, J. Appl. Phys. **66**, 4381 (1989).

[11] D. Bertram, H.T. Grahn, C. Van Hoof, J. Genoe, G. Borghs, W.W. Rühle, and K. von Klitzing, Phys. Rev. B **50**, 17309 (1994).

[12] J. Christen and D. Bimberg, Phys. Rev. B **42**, 7213 (1990).
[13] J.F. Young, B.M. Wood, G.C. Aers, R.L.S. Devine, H.C. Liu, M. Buchanan, A.J. Spring Thorpe, and P. Mandeville, Superlatt. Microstruct. **5**, 411 (1989).
[14] C. Van Hoof, E. Goovaerts, and G. Borghs, Phys. Rev. B **46**, 6982 (1992).
[15] L. Eaves, M.L. Leadbeater, D. G. Hayes, E.S. Alves, F.W. Sheard, G.A. Toombs, P.E. Simmonds, M.S. Skolnick, M. Henini, and O.H. Hughes, Solid-State Electron. **32**, 1101 (1989).
[16] M.S. Skolnick, P.E. Simmonds, D.G. Hayes, G.W. Smith, A.D. Pitt, C.R. Whitehouse, H.J. Hutchinson, C.R.H. White, L. Eaves, M. Henini, and O.H. Hughes, Phys. Rev. B **42**, 3069 (1990).
[17] C. Van Hoof, G. Borghs, and E. Goovaerts, Appl. Phys. Lett. **59**, 2139 (1991).
[18] T.S. Turner, L. Eaves, C.R.H. White, M. Henini, and G. Hill, Semicond. Sci. Technol. **9**, 552 (1994).